

Humidity-sensitive electrical response of sintered MgFe_2O_4

G. GUSMANO, G. MONTESPERELLI, P. NUNZIANTE, E. TRAVERSA
*Department of Chemical Sciences and Technologies, University of Rome "Tor Vergata",
Viale della Ricerca Scientifica, 00133 Rome, Italy*

Pellets of MgFe_2O_4 were prepared by sintering, at different temperatures, powders prepared either by solid-state reaction between MgO and Fe_2O_3 , or by the thermal decomposition of hydroxide mixtures, co-precipitated from magnesium and iron nitrate solutions with an Mg/Fe ratio of 1:2. Mercury porosimetry, specific surface area measurements and scanning electron microscopy were used in order to determine the main microstructural characteristics of the pellets. Electrochemical impedance spectroscopy (EIS) was used to correlate the humidity-sensitive electrical response of the pellets with their microstructure, in particular with total open porosity and pore-size distribution. EIS measurements showed a close correlation between their relative humidity dependence of the electrical resistance and the microstructure of the sintered bodies. Rather good reproducibility and a fast response time to humidity variations, evaluated from d.c. measurements, were also observed. These properties are also strictly dependent on the microstructure.

1. Introduction

Humidity sensors suitable for use in automated systems have been widely developed during recent years. Porous ceramics have been identified as candidates for use as sensing elements in humidity-measurement devices, because of their good mechanical characteristics and strong resistance to chemical attack, which determine their durability and measurement reproducibility [1, 2].

Spinel-type oxides have shown promising sensitivity and short response times [3-6]. Their electrical response, with impedance changes at different relative humidities, is due to physisorption and the capillary condensation of water molecules [7]. Therefore, the microstructure of porous compacts is primarily responsible for their humidity-sensitive electrical properties [7, 8]. Methods have already been proposed in the literature to control the microstructure of spinel-type materials, in order to improve their sensitivity to humidity variation [5, 9].

The aim of this work was to investigate the effect of the microstructural characteristics of sintered MgFe_2O_4 pellets on their electrical behaviour, studied by electrochemical impedance spectroscopy (EIS). Pellets were prepared by sintering at different temperatures MgFe_2O_4 spinel powders with different microstructures and reactivities.

2. Experimental procedure

2.1. Materials

Two sets of MgFe_2O_4 powders were prepared. The first powder (A) was obtained by solid state reaction at 1300°C between MgO and Fe_2O_3 (Carlo Erba RPE

reagents), whereas the second powder (B), was obtained by the thermal decomposition at 450°C of a hydroxide mixture, co-precipitated from a solution of magnesium and iron nitrates with an Mg/Fe atomic ratio stoichiometric to the spinel formation [10].

The powders were pressed at 20 MPa in the presence of an organic binder, into discs 12 mm diameter and 1 mm thick. Four different sets of specimens were prepared by sintering for 8 h in air the green bodies derived from the two powders: Specimens A1 and A2 were made up from powder obtained by solid-state reaction, sintered at 850 and 1100°C , respectively. Specimens B1 and B2 were obtained sintering at 750 and 850°C the powder from the thermal decomposition of hydroxides. Sintering temperatures were selected on the basis of the dilatometric measurements carried out on both the powders.

Gold electrodes, 10 mm diameter, were applied by vacuum evaporation on both sides of all the specimens, in order to carry out the electrical measurements.

2.2. Measurements

The pellets were analysed by the following techniques:

- (i) mercury porosimetry (Carlo Erba Instruments mod. 2000);
- (ii) specific surface area measurements with the BET method using nitrogen as adsorbate (Carlo Erba Instruments mod. Sorptomatic 1900);
- (iii) scanning electron microscopy (SEM) (Cambridge Stereoscan 360);
- (iv) electrochemical impedance spectroscopy (EIS): the spectra were collected in the range 10^{-2} - 10^5 Hz

using a Solartron 1255 frequency response analyser (FRA), equipped with a high-impedance adaptor to increase the input impedance of the instrument up to 10^{11} Ω . The tests were carried out at 40 °C and at relative humidity (RH) values ranging from 5%–85%, obtained by mixing dry and water-saturated air. Monitoring of RH was carried out using a Multisens Inc. hygrometric probe, which gave results accurate to within $\pm 2\%$;

(v) d.c. measurements: 1 V was applied to the specimens using a potentiostat PAR 273 and measuring the corresponding current to cyclic variation of RH from 5%–85%.

3. Results and discussion

3.1. Microstructural analysis

Table I lists the main microstructural characteristics of the starting powders. A detailed discussion of the powder analysis is given elsewhere [10].

Table II shows the main microstructural characteristics of the pellets. With increasing sintering temperature, a decrease of total open porosity and a shift of the pore-size distribution towards larger radii were observed. The sintering temperature does not seem to affect significantly the specific surface area.

Specimens prepared from Powder B, which are characterized by submicrometer particles, show higher specific surface areas, smaller pores and lower total open porosities than specimens prepared from Powder A.

Fig. 1 shows scanning electron micrographs of Specimens A2 and B1, representative of the extremes of microstructural morphology. Specimen A2 is made up of grains ranging from about 0.5–5 μm , while Specimen B1 is made up of uniform grains, about 50 nm in size.

3.2. Electrical analysis

Except in the case of the lowest RH, in which only one semicircle was observed, the typical impedance plot at different RH values shows two semicircles (Fig. 2).

TABLE I The main microstructural characteristics of the powders

	Powder A	Powder B
Specific surface area (BET) (m^2g^{-1})	1.5	116
Particle size (SEM) (μm)	0.5–10	< 0.1
Agglomerate size (SEM) (μm)	–	0.5–1

TABLE II Pore-size distribution (%) and specific surface area for the pellets

Sample	Porosity (%)		Pore-size distribution (%)					Specific surface area (mm ²) BET (m^2g^{-1})	
	Total open	Closed	< 3.8 nm	3.8–10 nm	10–20 nm	20–100 nm	100–500 nm		> 500 nm
A1	40.0	3.0	–	–	–	0.7	37.4	1.9	1.5
A2	15.5	12.8	–	0.2	–	–	9.1	6.2	1.5
B1	36.6	4.1	2.0	1.5	14.7	9.5	7.2	1.7	12.3
B2	26.4	5.8	–	–	7.8	11.4	5.1	2.1	12.1

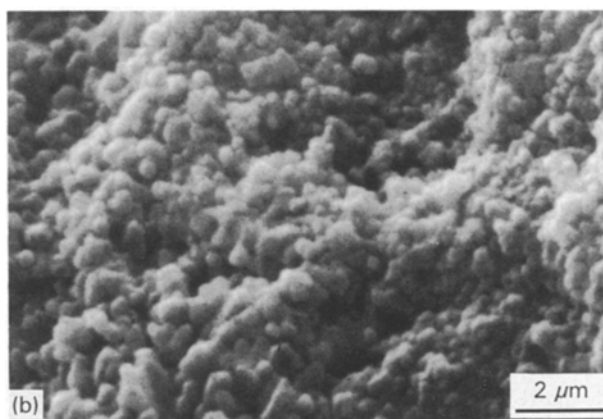
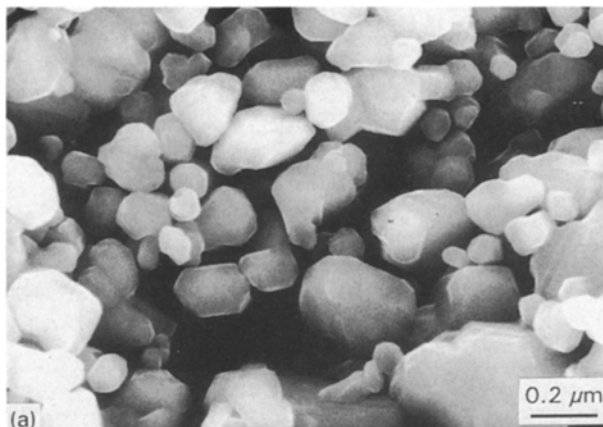


Figure 1 Scanning electron micrographs of the fracture surface of Specimens (a) A2 and (b) B1.

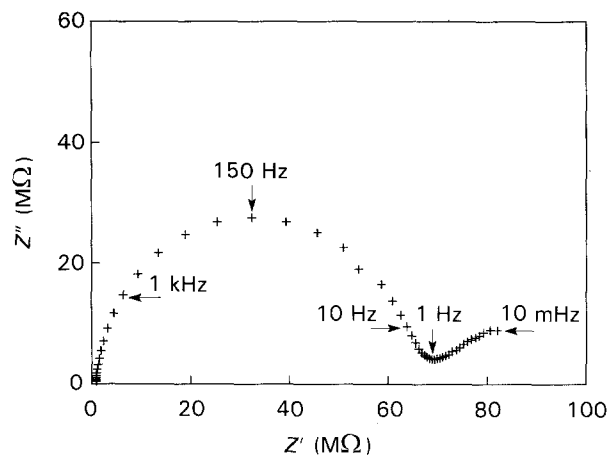


Figure 2 Complex impedance plot for Specimen B1, at 40 °C and 28% RH.

One, at low frequencies, is not complete and its centre is below the real axis. The second at higher frequencies is also inclined, it does not pass through the origin of the complex plane axes and its intercept with the real axis at high frequencies is independent of RH.

The results show that the same equivalent circuit proposed by Yeh *et al.* for other ceramic oxides [11], can also be used to describe the electrical behaviour of MgFe_2O_4 . The circuit is made up of a resistive element, ascribable to the crystal grain, and two RC elements, in series. The one at high frequencies is characteristic of the grain surface and that at low frequencies of the electrode polarization. The value of grain surface resistance, R_{gs} , has been calculated from the difference of the intercepts with the semicircle at high frequencies with the real axis in the complex plane. In some cases a circular fit interpolation was necessary, when an incomplete semicircle was detected.

The RH-dependence of R_{gs} , measured at 40 °C, is shown in Fig. 3. As a general trend, a decrease in R_{gs} was observed with increasing RH, which is characteristic of an ionic conduction mechanism. The electrical response of the different pellets to the variation of RH fits quite well with the results of the microstructural analysis. Both the total open porosity and the pore-size distribution influence the electrical behaviour. The lowest R_{gs} in the whole RH range, as measured on Specimens A1, is due to the highest total open porosity and to its size distribution mainly in the range 100–500 nm. A small number of pores in the range 20–100 nm allows the sample to exhibit good sensitivity at low RH.

Specimen A2 has the minimum open porosity, and thus the lowest resistance values at very low RH. The small open porosity also causes a smoother decrease in resistance with increasing RH up to about 40%. However, above 40% RH, the R_{gs} of Pellet A2 shows a strong RH-dependence. This behaviour can be explained in terms of the pore-size distribution of Specimen A2. The absence of pores having size which allows capillary condensation [12], explain the low

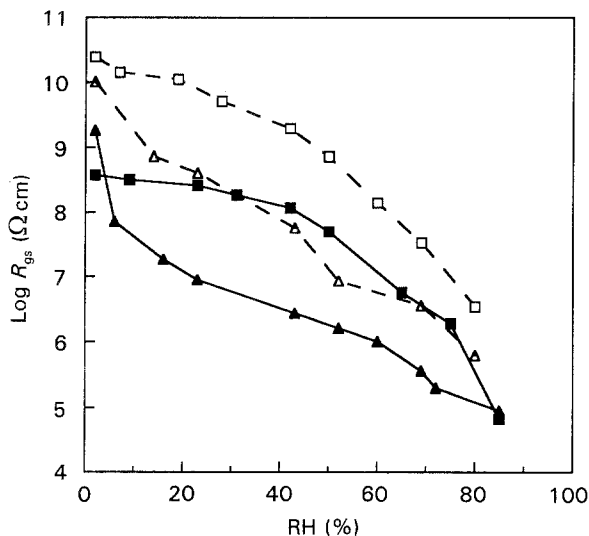


Figure 3 The RH-dependence of R_{gs} for the different specimens, at 40 °C. (▲) A1, (■) A2, (△) B1, (□) B2.

RH-sensitivity of R_{gs} below 40% RH and the good sensitivity at higher RH. The large number of pores larger than 500 nm, about 41% of the total, is responsible of the good sensitivity at high RH. Because these pores do not allow capillary condensation, only water adsorption can contribute to the conduction mechanism.

Specimens B1 and B2 have similar pore distribution, more uniform and spread on a wider range than Specimens A, and this explains that these specimens showed an RH-dependence closer to an exponential manner with respect to Specimens A, as shown in Fig. 3 [13].

In order to verify how the microstructure influences the electrical response, tests of reproducibility and time response were performed on the samples. The results for Specimens A2 and B1, corresponding to the extremes of microstructural features, are reported below.

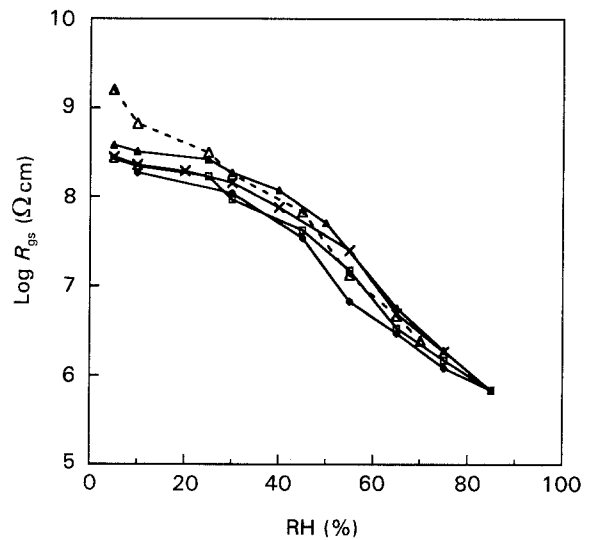


Figure 4 Log resistance versus RH curves for Specimen A2, measured at different time intervals. (▲) Initial, (□) 1 day, (◆) 2 days, (×) 4 days, (---△---) 5 days, heat cleaned.

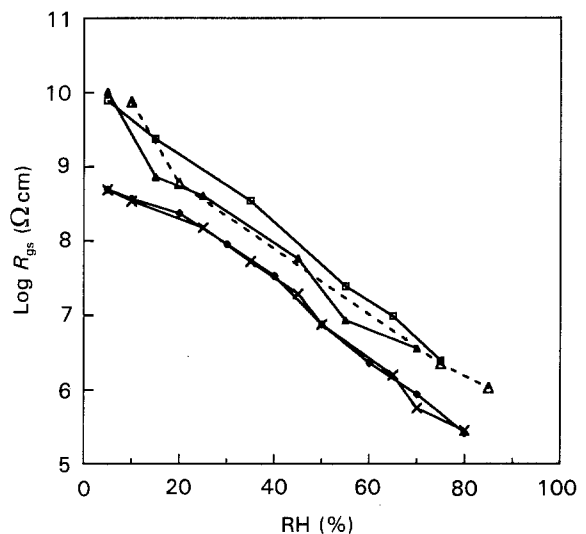


Figure 5 Log resistance versus RH curves for Specimen B1, measured at different time intervals. (▲) Initial, (□) 1 day, (◆) 3 days, (×) 4 days, (---△---) 5 days, heat cleaned.

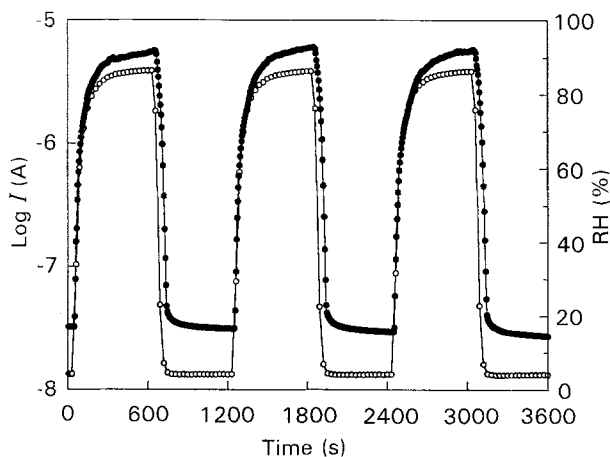


Figure 6 Effect of (○) RH cycling on (●) the current response for Specimen A2.

The results of reproducibility tests are plotted in Figs 4 and 5. Tests were carried out maintaining the sample at 5% RH for different periods (12–48 h) or at 400 °C for 1 h before each set of measurements. The good reproducibility shown by Specimen A2 (Fig. 4), independently from the measurement cycle, is attributable to the presence of large pores, while the response of Specimen B1 (Fig. 5) is still quite good but more affected by the measuring cycle, due to the presence of small pores which make the release of water at low RH more difficult.

Even more interesting are the response time results obtained on the same specimens, as reported in Fig. 6 for Specimen A2, and in Fig. 7 for Specimen B1. Once again, Specimen A2 shows the best behaviour: current variations follow the RH variation very well. The response time under experimental conditions can be estimated as low as a few seconds and no appreciable drift is observed. Much slower is the response of Specimen B1 to RH variations. It can be estimated in the order of minutes, and a drift of the measured current has been observed at the end of each cycle.

4. Conclusion

The microstructural features influence the electrical behaviour of porous pellets of MgFe_2O_4 and their sensitivity to humidity. The microstructure of the starting powder has a great influence on the final characteristics of the pellets. The total open porosity and its distribution play a dominant role. Our results demonstrate that uniform pore-size distribution is associated with good sensitivity. Because the mechanism of ionic conduction, due to physisorption of water molecules on the oxide surface, is greatly assisted by capillary condensation, a wide pore-size distribution is desirable to permit also the occurrence of capillary condensation over a wider humidity range. At the same time, the presence of small pores causes not fully reproducible behaviour, some drift and slower response of the sensors.

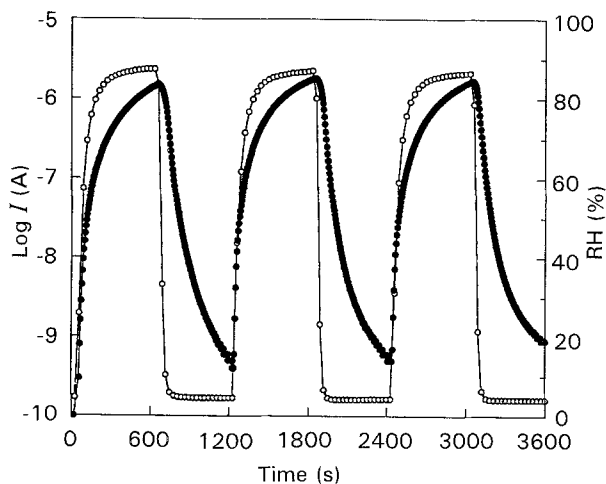


Figure 7 Effect of (○) RH cycling on (●) the current response for Specimen B1.

Acknowledgement

This work was supported by the Italian National Research Council (CNR), under the auspices of the Targeted Project "Special Materials for Advanced Technologies".

References

1. B. M. KULWICKI, *J. Am. Ceram. Soc.* **74** (1991) 697.
2. H. ARAI and T. SEIYAMA, in "Sensors: A Comprehensive Survey, Chemical and Biochemical Sensors, Part II", Vol. 3, edited by W. Göpel, J. Hesse and J. N. Zemel (VCH Verlag, Weinheim, 1992) p. 981.
3. T. NITTA, Z. TERADA and S. HAYAKAWA, *J. Am. Ceram. Soc.* **63** (1980) 295.
4. T. SEIYAMA, N. YAMAZOE and H. ARAI, *Sens. Actuators* **4** (1983) 85.
5. T. SUZUKI and N. MATSUI, in "Analytical Chemistry Symposia Series: Chemical Sensors", Vol. 17, edited by T. Seiyama, K. Fueki, J. Shiokawa and S. Suzuki (Kodansha, Tokyo, and Elsevier, Amsterdam, 1983) p. 381.
6. G. GUSMANO, G. MONTESPERELLI, P. NUNZIANTE and E. TRAVERSA, in "Ceramic Transactions: Ceramic Powder Science IV", Vol. 22, edited by S. I. Hirano, G. L. Messing and H. Hausner (American Ceramic Society, Westerville, Ohio, 1991) p. 545.
7. Y. SHIMIZU, H. ARAI and T. SEIYAMA, *Sens. Actuators* **7** (1985) 11.
8. K. KATAYAMA, K. HASEGAWA, T. TAKAHASHI, T. AKIBA and H. YANAGIDA, *ibid.* **A24** (1990) 55.
9. H. T. SUN, M. T. WU, P. LI and X. YAO, *ibid.* **19** (1989) 61.
10. G. GUSMANO, P. NUNZIANTE, E. TRAVERSA and R. MONTANARI, *Mater. Chem. Phys.* **26** (1990) 513.
11. Y. C. YEH, T. Y. TSENG and D. A. CHANG, *J. Am. Ceram. Soc.* **73** (1990) 1992.
12. H. JANKOWSKA, H. SWIATKOSKI and J. CHOMA, "Active Carbon" (Ellis Horwood, Chichester, 1991) p. 121.
13. G. GUSMANO, G. MONTESPERELLI, P. NUNZIANTE and E. TRAVERSA, *Br. Ceram. Trans.* **92** (1993) 104.

Received 1 December 1992
and accepted 2 April 1993